Received: 14 May 2019 | Accepted: 12 November 2019

DOI: 10.1002/hyp.13652

RESEARCH ARTICLE

WILEY

Spatial and temporal variations in the groundwater contributing areas of inland wetlands

Junehyeong Park[1] | Dongdong Wang[2] | Mukesh Kumar[1]

[1]Department of Civil, Construction, and Environmental Engineering, University of Alabama, AL, USA

[2]Department of Computer Science, University of Central Florida, AL, USA

Correspondence
Email: mukesh.kumar@ua.edu

Funding information
National Science Foundation, Grant/Award Numbers: EAR-1856054, EAR-1920425

Abstract

Water quality and groundwater dynamics in wetlands are strongly influenced by the spatiotemporal distribution of contaminant application, and variations and changes in climate, vegetation, and anthropogenic interventions in its neighborhood. For groundwater-fed wetlands, this relevant neighborhood at least extends to the groundwater contributing area (GCA) boundary. In spite of its importance, understanding of the nature of GCA dynamics vis-à-vis meteorological variations remains largely understudied. This work attempts to map GCA of inland forested wetlands. Following that, two specific questions are answered: (a) Is GCA extent and its variation different than that of the topographic contributing area (TCA)? and (b) Is the temporal dynamics of GCA for different wetlands, all of which are experiencing very similar climatological forcing, similar? Our results show that GCAs for wetlands vary temporally, are much different in extent and shape than the TCA, and on an average are larger than the TCA. Although wetlands in the studied watershed experienced similar meteorological forcings, their covariation with forcings varied markedly. Majority of the wetlands registered an increase in GCA during dry period, but for a few the GCA decreased. This highlights the role of additional physical controls, other than meteorological forcings, on temporal dynamics of GCA. Notably, wetlands with larger TCA are found to generally have larger average GCA as well, thus indicating the dominant role of topography in determining the relative size of average GCA over the landscape. Our results provide a refined picture of the spatiotemporal patterns of GCA dynamics and the controls on it. The information will help improve the prediction of wet period dynamics, recharge, and contamination risk of groundwater-fed wetlands.

KEYWORDS
Wetland, Contributing area, Groundwater, Hydrologic modeling

1 | INTRODUCTION

Wetlands provide a multitude of ecosystem services (Barbier, 1993; Bullock & Acreman, 2003; Mitsch & Gosselink, 2000; Richardson, 1994; Zhu et al., 2017), including groundwater recharge (McCarthy, 2006), flood control (Galat et al., 1998; Hey & Philippi, 1995; Watson, Ricketts, Galford, Polasky, & O'Niel-Dunne, 2016), water quality buffering (Gilliam, 1994) through removal of carbon (Reuter, Djohan, & Goldman, 1992), metals (Mungur, Shutes, Revitt, & House, 1995), sediments (Jordan, Whigham, Hofmockel, & Pittek, 2003), and nitrate (Lin, Jing, Wang, & Lee, 2002), and provisioning of aquatic habitat for a number of plant and animal life (Benson, Carberry, & Langen, 2018; Knight, 1997; Knight, Clarke, & Bastian, 2001; Zedler & Kercher, 2005). Given their importance to varied life forms including humans, it is important to understand the controls on wetland dynamics so as to predict their sustainability and function.

Hydrologic dynamics in wetlands are strongly influenced by the variations and changes in climate (Erwin, 2009; Fossey & Rousseau, 2016; Liu & Kumar, 2016; Zhu et al., 2017), bathymetry (Bertassello, Rao, Park, Jawitz, & Botter, 2018; Park, Botter, Jawitz, & Rao, 2014), vegetation, and anthropogenic interventions (Krapu, Kumar, & Borsuk, 2018; Van Meter & Basu, 2015). These factors alter the wetland dynamics by modulating the recharge to wetlands, which can be from groundwater (Harbor, 1994; Hunt, Krabbenhoft, & Anderson, 1996; Jolly, McEwan, & Holland, 2008; Min, Perkins, & Jawitz, 2010; van der Kamp & Hayashi, 2009; Winter, 1999), surface runoff (Ameli & Creed, 2017; Harbor, 1994; Jolly et al., 2008; Vanderhoof, Alexander, & Todd, 2016; Winter, 1999) and direct precipitation on it. As groundwater and surface water recharge affects the wetland dynamics, it is likely that changes in forcings and properties within the contributing area of surface water and groundwater will affect wetland's wet period and water quality. Unsurprisingly, several studies have discussed the dynamics of surface water contributing area of wetlands, especially in prairie pothole settings where closely distanced wetlands can merge and split over time (Chu, Yang, Chi, & Zhang, 2013; Shaw, Vanderkamp, Conly, Pietroniro, & Martz, 2012; Yang & Chu, 2013) thus affecting contributing areas as well. In these studies, surface water contributing area have been often discussed in terms of hydrologic connectivity. The dynamics of groundwater contributing area (GCA) of wetlands, however, remains mostly understudied in part due to the challenges associated with observing groundwater field at fine spatiotemporal resolutions.

One of the few studies focused on groundwater contributing area dynamics of wetlands was performed by O'Driscoll & Parizek (2003), who used a detailed groundwater monitoring network with 124 nested piezometers at 31 locations (each location contained 4 piezometers at depths 1.5, 3.0, 6.1, and 9.1 m) to map hydrologic catchments for a chain of karst wetlands in central Pennsylvania. The study showed that the maximum surface flow contributing area or the topographic catchment areas (TCAs) of karst wetlands were generally larger than the effective groundwater contributing areas. Furthermore, the observations indicated that the groundwater contributing areas are dynamic and vary across seasons. Locke et al. (2005) used a multitude of existing groundwater-level data to obtain GCAs by identifying areas hydraulically upgradient of the site using flownet analyses. They generated GCA for 12 Illinois Nature Preserves and other natural areas. The report concluded that because of paucity of groundwater observations at fine spatial scales, alternative data and methods should be developed, especially considering that GCA is expected to be dynamic as a result of fluctuations in recharge and water usage (e.g., variations in climatic conditions, alterations to surface permeability, and increased or decreased pumping). They also noted data-centric methods based on historical data may be inaccurate for evaluations in the future as the hydraulic conditions are dynamic.

The challenge posed by the need for fine resolution groundwater gauge network to map GCA and predict its dynamics in near-term and future can be alleviated through the use of adequately calibrated and validated distributed surface-subsurface hydrologic models such as Parflow, FIHM, PIHM, Hydrogeosphere, and PAWS (Kollet & Maxwell, 2006; Kumar, Duffy, & Salvage, 2009; Qu & Duffy, 2007; Shen & Phanikumar, 2010; Therrien, McLaren, Sudicky, & Panday, 2010) that can potentially account for the dynamic contributions of surface and groundwater recharge in space and time. To our knowledge, no such model application has been performed yet to obtain temporally varying GCA of wetlands. One reason for the lack of such a study could be the computational demand associated with the application of distributed surface-subsurface hydrologic models. These applications are generally computationally intensive to begin with (Hwang, Park, Sudicky, & Forsyth, 2014; Kumar & Duffy, 2015; Vivoni et al., 2011) and are likely to be so in settings where wetlands are small (area < 0.5 km^2), thus requiring fine resolution simulations over the model domain. Misut and Monti (2016) did map long-term or static groundwater watersheds of 48 surface water bodies on the Long Island, New York. They used MODFLOW-2005 (Harbaugh, 2005) to simulate groundwater field for a period ranging from 1968 to 1983 and then used MODPATH version 6 (Pollock, 2012) to trace particles on the groundwater field to obtain static delineations of groundwater watersheds. Nippgen, Mcglynn, and Emanuel (2015) evaluated spatial and temporal variations in contributing areas using a parsimonious but fully distributed rainfall-runoff model, WECOH (Watershed ECOHydrology). The study used empirical data about network connectivity from water table observations from 84 shallow groundwater wells in the watershed to evaluate the fraction of groundwater storage that may be contributing to a stream. Although this study is one of the few that provided a dynamic mapping for groundwater contributing area, the evaluation was performed only for streams instead of wetlands.

Building on the aforementioned studies, this work first mapped the temporally evolving GCA of freshwater inland wetlands. Following that, two specific questions were answered: (a) Is GCA extent and its variation different than that of TCA? (b) Is the temporal dynamics of GCA for different wetlands, all situated in close proximity and experiencing very similar climatological forcing, similar? To answer these questions, a physically-based, fully distributed hydrologic model PIHM (Kumar, 2009; Qu & Duffy, 2007) was implemented in the Second Creek watershed in southwest North Carolina. GCA was derived for multiple wetlands within the study area using the simulated groundwater field. Section 2 provides details of the study site, the hydrologic model, and the method to delineate GCA of wetlands. Section 3 discusses our findings and answers the questions mentioned above. Section 4 summarizes the major results and conclusions, discusses the limitations, and suggests future directions of research.

2 | DATA AND METHOD

2.1 | Site Description

The study was conducted in the Second Creek watershed in southwest North Carolina (Figure 1). The watershed is a part of South Yadkin river basin that drains 325 km^2 area at USGS streamflow gauge # 02120780 (35.6 N, 80.7 W) located on the Second Creek. Streamflow at the gauge has been measured for more than thirty years. The

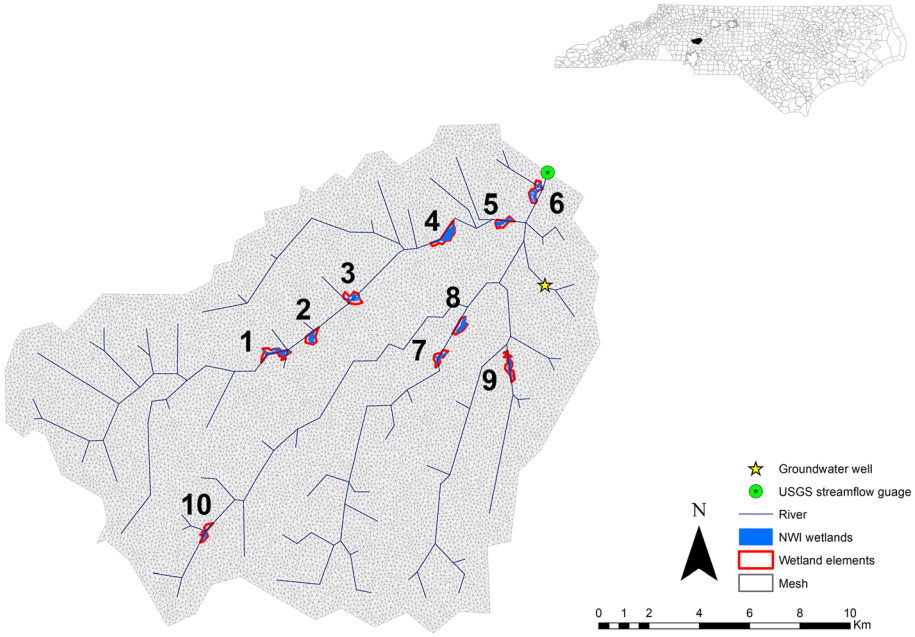

FIGURE 1 Second creek watershed with the distribution of the wetlands (of a size larger than 57000 m2) based on the National Wetland Inventory data (https://www.fws.gov/wetlands/) including model grids used for this research. Also shown are the USGS gauging stations and streamflow network. The dark-colored polygon in the North Carolina map (shown in the upper right corner) represents the location and extent of the Second Creek watershed

watershed also has a USGS groundwater gauging station (#354057080362601) where daily groundwater level has been measured since 1989. The watershed was selected because it contains multiple forested freshwater wetlands within its boundary. Physiography of the watershed is characterized by valleys and ridges oriented along the southwest-northeast direction. The elevation in the watershed ranges from 197 to 331 m. Land cover in the watershed mainly consists of hay/pasture (37.6%), deciduous forest (32.9%), developed area (6.8%), and evergreen forest (5.4%). The most common soil types in the watershed are loam in the riverbed and riparian regions and sandy clay loam in the uplands. Based on the Koppen-Geiger climate classification (Kottek, Grieser, Beck, Rudolf, & Rubel, 2006), the watershed falls in a warm temperate climate zone characterized by humid and warm summer. The average temperature in the watershed during 1981-2013 was 15.5 °C and the annual precipitation ranged from 703 to 1473 mm. The watershed consists of several inland wetlands, the majority of which are classified as freshwater forested/shrub wetland or freshwater pond according to the National Wetland Inventory data (U.S. Fish and Wildlife Service, 2019). Because of the computational constraint associated with ensuing analyses, here we focused our attention on the largest ten wetlands in the watershed with area ranging from 57,000 to 167,000 m^2. Type and attribute of each of these wetlands are listed in Table S1.

2.2 | Hydrologic model application

2.2.1 | Model Description

A physically based, fully distributed hydrologic model, PIHM (Kumar, 2009; Qu & Duffy, 2007) was used to simulate coupled hydrologic states and fluxes. Processes simulated in PIHM include snowmelt, evapotranspiration (Penman-Monteith equation), interception (Rutter model), overland flow (2D diffusion-wave equation), unsaturated zone infiltration (a 1D approximation of the Richards equation), groundwater flow (Boussinesq equation), and streamflow (1D diffusion-wave equation). The model couples surface (channel routing and overland flow) and subsurface (groundwater and unsaturated flow) process based on continuity of fluxes across grid interfaces while ensuring the mass conservation locally and globally. Using a semidiscrete finite-volume approach, the model spatially discretizes the partial differential equations of hydrologic states into ordinary differential equations (ODEs). The system of ODEs defined on all mesh elements is assembled and solved simultaneously in time using a stiff solver based on Newton-Krylov iteration. An adaptive time-stepping scheme is used to capture the varied time scales of states. The model has been previously applied at multiple scales and in diverse hydro-climatological settings for simulating coupled dynamics of streamflow, groundwater, soil moisture, snow, and evapotranspiration fluxes (Chen, Kumar, & McGlynn, 2015; Chen, Kumar, Wang, Winstral, & Marks, 2016; Kumar, Marks, Dozier, Reba, & Winstral, 2013; Seo, Sinha, Mahinthakumar, Sankarasubramanian, & Kumar, 2016; R. Wang, Kumar, & Marks, 2013; Yu, Duffy, Baldwin, & Lin, 2014; Zhang, Chen, Kumar, Marani, & Goralczyk, 2017). The model has already been used to study wetland dynamics in multiple studies (Liu & Kumar, 2016; D. Wang, Liu, & Kumar, 2018; Yu et al., 2015).

2.2.2 | Domain discretization

The entire watershed, including the inland forested wetlands, was discretized using unit elements that are triangular in 2D and prismatic in 3D. Streams were discretized using linear-shaped unit elements that are rectangular in 2D and cuboidal in 3D. These elements were projected downward to the bedrock (for land surface elements) or the river bed (for river elements), respectively (Kumar, 2009). Each land element was discretized into four layers: a top surface overland flow

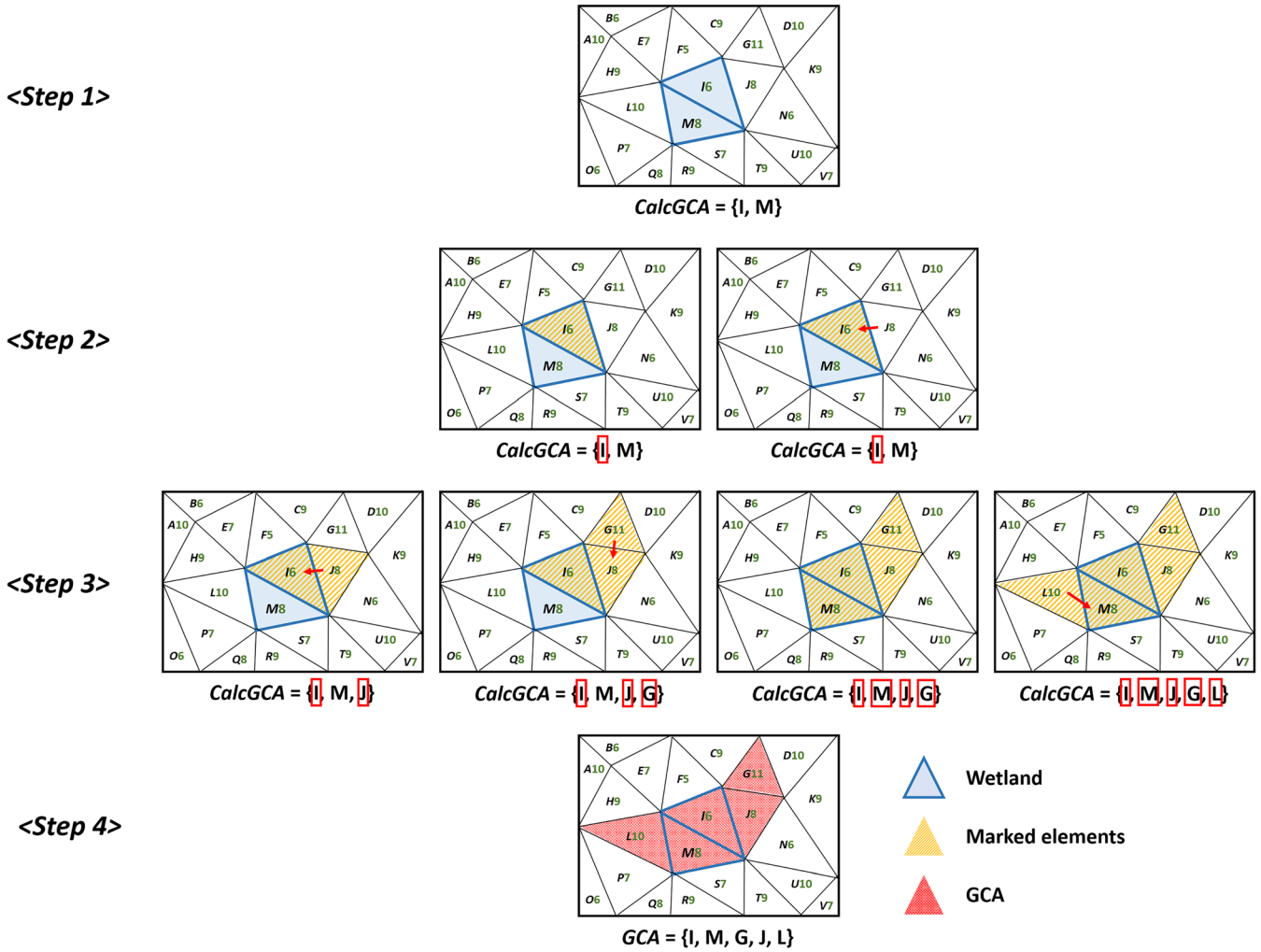

FIGURE 2 Conceptual diagram explaining the delineation steps of groundwater contributing area for a twocell wetland. Sub-steps sequence is from left to right. Letters and numerals on each triangle element indicate its name and centroidal elevation respectively. Marked elements are identified by orange colored shade and also using hollowed red rectangles. Arrow indicates the act of adding an element to the set CalcGCA

layer with variable thickness, a relatively thin unsaturated layer with a defined maximum thickness *T* (default value of *T* is 0.25 m), a second unsaturated layer that extends from *T* to groundwater level, and a groundwater layer. Moisture content in both unsaturated layers could range from full saturation to residual saturation. The two lowest layers had variable dimensions, as their thickness depended on the evolving groundwater table depth. Each river unit was vertically discretized into two layers, with a flowing river on the top and a groundwater zone below it. As the average combined thickness of soil, saprolite, and the transition zone of regolith has been estimated to be less than 20 m in the piedmont region of North Carolina (Daniel, 1987; Zhang et al., 2017), a uniform depth of 20 m was considered as the lower boundary of the subsurface layer. Use of triangular cells allowed efficient and accurate representation of physiographic, climatic and hydrographic features because of their spatial adaptivity and ability to conform to sinuous boundaries (Kumar, Bhatt, & Duffy, 2009; Kumar, Duffy, et al., 2009; Vivoni, Ivanov, Bras, & Entekhabi, 2004; D. Wang et al., 2018). As all major wetlands in the watershed were smaller than 167,000 m^2 in area, capturing groundwater dynamics required modeling at fine spatial-temporal resolution. Here, the simulation was conducted for a discretization with 25443 elements. The discretization was generated using the PIHMgis (Bhatt, Kumar, & Duffy, 2014) while enforcing a maximum area constraint of 20,000 m^2, i.e., all Delaunay triangles in the domain were of size smaller than or equal to 20,000 m^2.

2.2.3 | Model parameterization

Model parametrization over each grid was obtained using the PIHMgis, which facilitates automatic extraction and assignment of ecological and hydrogeological parameters and meteorological forcings on each discretization grid using a shared data model (Kumar, Bhatt, & Duffy, 2010). Derived model parameters describe topography, soil, land cover, vegetation, geology, and meteorology. We used the 30 m resolution elevation data from National Elevation Dataset (NED) (Gesch et al., 2002), USDA-NRCS Soil Survey Geographic (SSURGO) soil data (Soil Survey Staff, Natural Resources Conservation

Service, 2005), and National Land Cover Dataset (NLCD) land cover data (Homer et al., 2015). Meteorological forcings such as precipitation, air temperature, relative humidity, wind speed, and radiation were obtained from the North America Land Data Assimilation System Phase 2 (NLDAS-2) data (Xia et al., 2012), which has a spatial and temporal resolution of 1/8 degree and an hour, respectively. As detailed geologic data in the watershed was unavailable, following the lead of other studies (Abdelbaki, 2016; Rodríguez-Lado, Rial, Taboada, & Cortizas, 2015; Wösten, Pachepsky, & Rawls, 2001) spatial distribution of geological properties were approximated based on SSURGO soil map. Pedotransfer functions (Wösten et al., 2001) were used to assign the properties, which were later modified uniformly across the watershed during calibration.

The model simulation was conducted for six water years ranging from Sep 1st, 2004 to Aug 31th 2010. A water year is an annual period spanning from the start of September to the end of August of next year. The simulation was performed using the calibration parameters derived in Liu and Kumar (2016). Initial conditions of hydrologic states on 09/01/2004 mid-night were also extracted from the same study. To map the states from the mesh configuration used in Liu and Kumar (2016) to that used here, Inverse Distance Weighted (IDW) interpolation was employed. To negate the effects of errors introduced by the IDW interpolation scheme and mismatch of a mesh configuration, the first year simulation was used to allow the system to equilibrate with the forcing. The one-year simulation length for "equilibration" was found to be sufficient for this watershed and was derived by comparing results from alternative simulations of varying lengths ranging from 3 months to 2 years. Only the simulation for the next five years (Sep 1st, 2005 to Aug 31th 2010) was used for analyses. It is to be noted that the average annual precipitation during 2005-2010 was equal to 1047 mm, which was close to the long-term average precipitation (1084 mm during 1979-2014) at the site. Also, the selected years had diverse climatology with the wettest water year (2009) receiving 1376 mm of precipitation while the driest water year (2006) receiving 869 mm. This provided the opportunity to study groundwater contributing area dynamics under a range of hydroclimatological conditions. Validation of the simulation results against gauged data of streamflow and groundwater table has already been presented in D. Wang et al. (2018); readers may consult the fine-scale scenario shown in Figure 3 of the referred text.

2.3 | Delineation of groundwater contributing area

The groundwater contributing area (GCA) for a given triangular element or set of elements (that could be representing a wetland) was obtained based on the classic multiple flow direction methods often used to delineate catchments for topography grids (e.g., Freeman, 1991; Quinn, Beven, Chevallier, & Planchon, 1991). However, the model domain discretization used here presented two challenges. First, the discretization used in PIHM is unstructured, with both triangular and linear unit elements. Second, each triangle has three neighbors (could be three triangles or at most two river reaches). Relevant

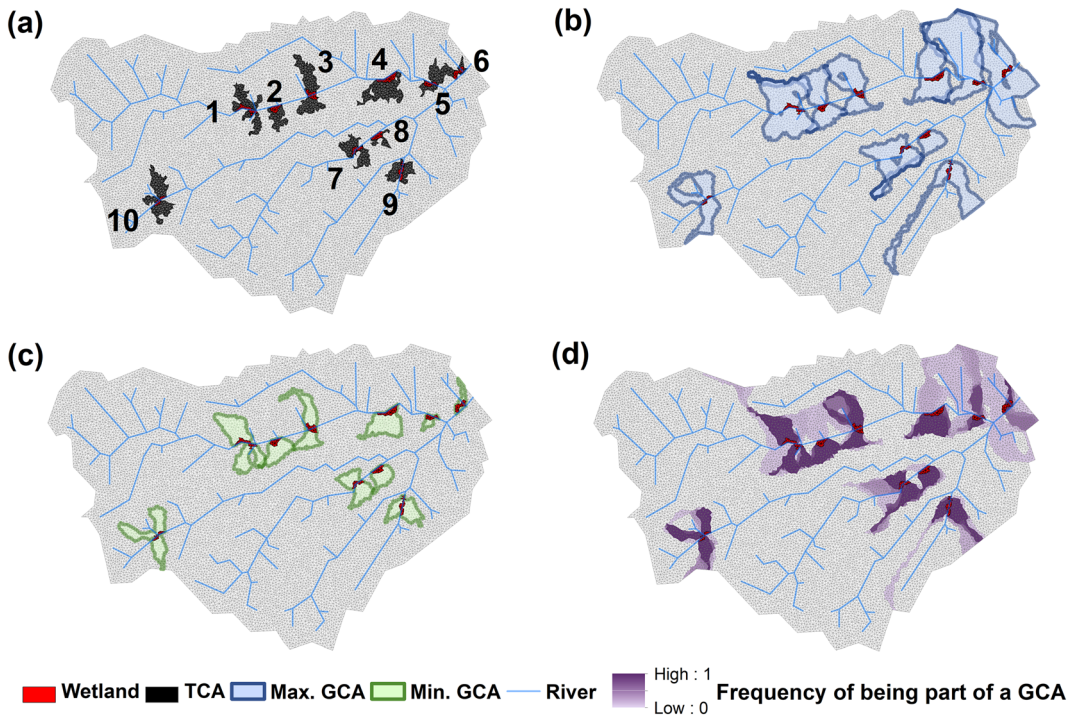

FIGURE 3 Topographic contributing area (TCA) (a), and maximum (b) and minimum (c) groundwater contributing area (GCA) for the ten wetlands in Second Creek watershed. The frequency with which a triangular element is part of GCA of a given wetland is shown in (d). Overlaps in the shown contributing areas of different wetlands are because they occur at different times during the simulation period

adjacency was considered for evaluation of groundwater connectivity between elements. The direction of connectivity was assigned based on flow direction at a given time step, which in turn was evaluated using the hydraulic gradient between an element and its neighbors. Steps for delineating the contributing area are as follows:

Step 1. Identify contiguous unit elements for which contributing area is to be evaluated. In the present context, these elements belong to a given target wetland. Push these elements into a list (/array) called CalcGCA.

Step 2. Select an element from CalcGCA and mark it. Then compare the groundwater elevation (GE) in it with three of its neighbors. If the neighboring element is not within the target wetland and GE in the neighboring element is higher than or equal to it, the neighbor is pushed into CalcGCA after checking that it is not already in there.

Step 3. Run step 2 for all unmarked elements in the CalcGCA, including elements added in the previous step, until there are none left.

Step 4. If all elements in the list are marked by now, the GCA is set as the collection of all elements, except the wetland cells, in the CalcGCA.

Step 5. Run steps 1-4 for contiguous unit elements belonging to other target wetlands for which contributing area is desired.

Figure 2 explains the implementation of these steps on a simple mesh. This study implemented the above steps for each wetland at each simulation time step. If instead of groundwater elevation in step 2 topographic elevation is considered, then the contributing area derived using the above algorithm will be the topographic contributing area (TCA). It is to be noted that GCA was derived for model-detected wetlands in this study. The model-detected wetlands were locations with simulated groundwater table being higher than -0.3 m for at least two continuous weeks in the growing season every other year. This definition for wetland conforms with National Research Council's definition of wetlands (National Research Council, 1995), and was used to delineate wetlands within the watershed in an earlier study (Liu & Kumar, 2016).

3 | RESULTS AND DISCUSSION

3.1 | Spatio-temporal variability of Groundwater Contributing Area (GCA) compared with Topographic Contributing Area (TCA)

GCA and TCA were obtained using the algorithm outlined in section 2.3. Assuming negligible changes in the land surface elevation in the watershed due to sediment erosion/deposition processes or geological activity during the simulation period, the TCA for different wetlands remained constant in time. In contrast, GCA for wetlands varied temporally, with a mean coefficient of variation (CV) of 0.28. CV for wetlands 5 and 6 are as large as 0.54 and 0.97, respectively (Table 1). Notably, both the TCA and GCA of wetlands varied spatially. TCAs of wetlands were different from each other (see Table 1, Figure 3) because of the differences in topographic configuration around them that majorly determines the surface flow field. Spatial variations in GCA of wetlands were due to dissimilarity in the groundwater field around wetlands, which in turn is an integrated response to local net recharge and lateral groundwater flow. The GCA was very different in shape w.r.t. the TCA (Figure 3). The temporal variations in the GCA were due to spatiotemporal fluctuations in the groundwater flow field. On average, GCAs were found to be much larger than TCAs for all wetlands (Table 1) in contrast to the result reported in O'Driscoll & Parizek (2003).

Figure 3 shows the maximum and minimum extent of GCA for ten wetlands during the simulation period. The difference between GCA and TCA varied across wetlands. For example, the average GCA for wetland 8 was larger by around 233% of the TCA, while the

TABLE 1 Topographic contributing area (TCA) and groundwater contributing area (GCA) of the 10 wetlands in the Second Creek watershed for the 5-year simulation period. SD indicates the standard deviation; CV indicates the coefficient of variation

	TCA (m^2)	Average of hourly GCA (m^2)	Maximum of hourly GCA (m^2)	Minimum of hourly GCA (m^2)	100*(GCA-TCA)/TCA	SD of hourly GCA (m^2)	CV of hourly GCA	% time when GCA>=TCA
Wetland 1	2,535,641	5,337,374	8,999,413	4,368,294	110.49	490,254.45	0.09	100.00
Wetland 2	1,228,643	2,023,327	5,713,509	1,840,571	64.68	92,910.17	0.05	100.00
Wetland 3	3,104,659	4,402,699	5,306,321	2,817,373	41.81	630,325.53	0.14	97.00
Wetland 4	2,922,320	3,388,735	5,951,742	2,648,004	15.96	880,257.59	0.26	80.07
Wetland 5	1,743,966	2,347,352	11,557,904	425,315	34.60	1,270,012.17	0.54	78.42
Wetland 6	678,688	1,824,312	12,147,632	578,622	168.80	1,767,067.03	0.97	68.00
Wetland 7	1,893,404	3,574,669	5,506,334	2,220,056	88.80	760,680.17	0.21	100.00
Wetland 8	636,532	2,117,044	2,999,076	1,322,807	232.59	563,425.90	0.27	100.00
Wetland 9	1,620,928	2,925,646	5,544,843	2,069,374	80.49	531,470.93	0.18	100.00
Wetland 10	2,857,660	3,747,364	4,871,311	3,220,590	31.13	340,164.41	0.09	100.00

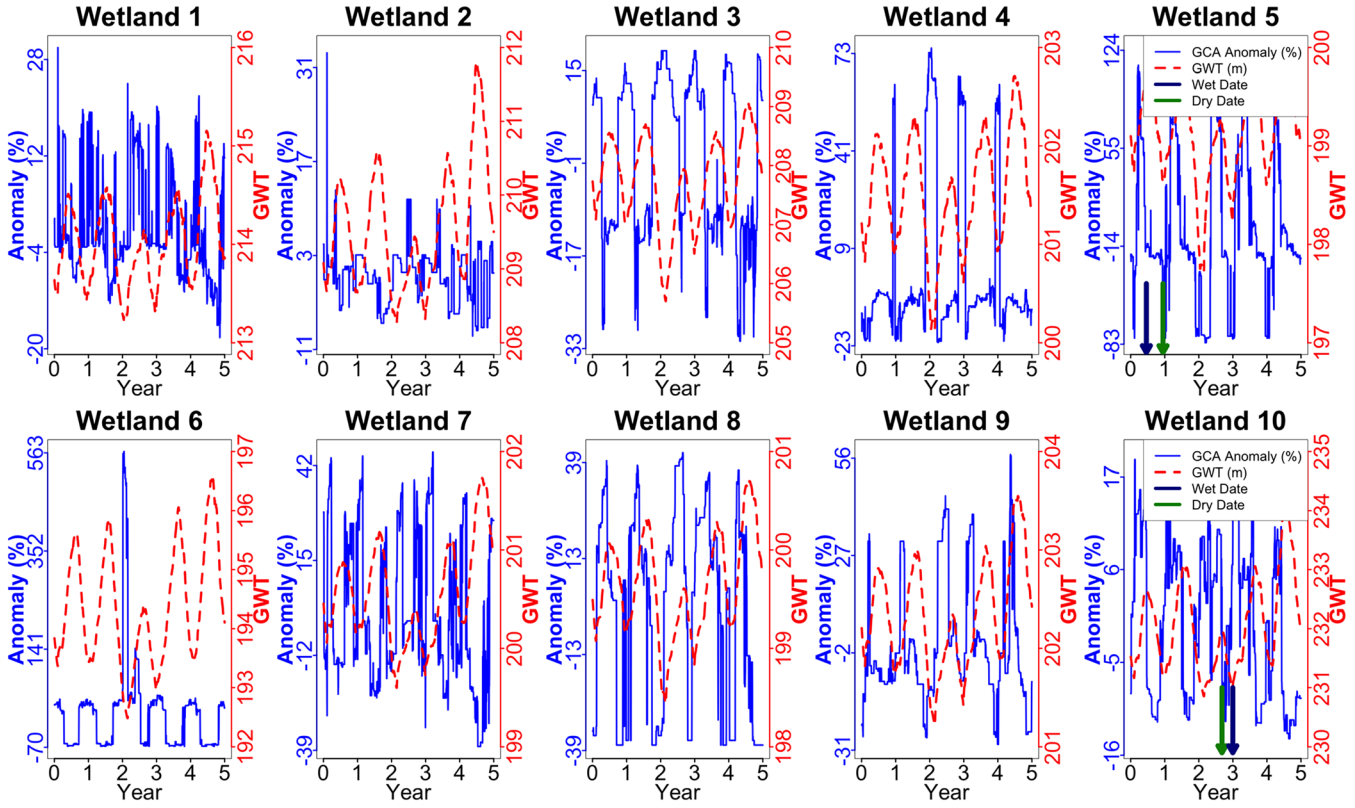

FIGURE 4 GCA anomaly and average groundwater table elevation for each wetland. The anomaly time series of GCA is calculated based on the percentage deviation from the mean of the GCA over the five simulation years. "0" on the horizontal axis represents Sep 1st 2005

corresponding magnitude of wetland 4 was only 16%. GCAs for different wetlands did sometimes get smaller than TCA (~7.6% of the simulation time). However, during these periods, GCA was smaller than TCA by 18.8 %. In contrast, during the period GCA was larger than TCA, on the average GCA was larger by 95.7 %. This indicates that for times when GCA was smaller than TCA, it was by a much smaller amount. Larger GCA than the TCA during most periods was because of the milder spatial gradient of the groundwater flow field relative to the topography, especially around the wetlands as they generally lie in flatter topographic areas that serve as groundwater flow convergence zones.

The differences between GCA and TCA were attributable to multiple factors including topographic configuration around wetlands, and other physiographic descriptors such as vegetation, soil and geology types that influence the spatial distribution of net recharge and lateral groundwater flow, and eventually the groundwater field. The Pearson correlation coefficient and the Spearman rank-order correlation coefficient between the average GCA and TCA was equal to 0.81 and 0.83, respectively. Both correlation coefficients were large enough to conclude there is a significant linear and monotonic relation between GCA and TCA. The result indicated that wetlands with larger TCA were likely to have larger GCA as well, thus highlighting topography's dominant role in determining the relative size of GCA for different wetlands over the landscape.

3.2 | GCA dynamics via-a-vis climatological variations

The time series of the extent of GCA variation w.r.t. the long term mean (i.e., mean for the entire simulation period), hereafter called the GCA anomaly, showed significant fluctuations in GCA at both event and seasonal scales (Figure 4). This was in contrast to mean groundwater dynamics in respective wetlands, which showed relatively smoother seasonal cycles. On average, GCA varied by 0.16, 1.296, 14.197, and 23.995 % at hourly, daily, monthly, and seasonal interval. In contrast, corresponding variations in GWT in wetlands were 0.007, 0.167, 4.268, and 10.382 % respectively. The reason for high-frequency variation in GCA anomaly, especially at finer temporal scales, was because even small changes in the groundwater table at the boundary of GCA at a given time step could (dis)connect groundwater table in neighboring areas thus contracting/extending the GCA significantly. This could also result in non-linear variations in GCA at both inter-event and inter-annual scales. For example, GCA anomaly in wetland 6 oscillated between around -70 % to 60 %, but it suddenly increased to 566.07 % in the 3rd year of the simulation (Figure 4). This abnormal fluctuation was because of the merging of existing GCA with a large neighboring area that drains into it during an extremely dry period.

An appreciable correlation existed between groundwater dynamics and GCA at the seasonal scale (Table 2). This was because, during

TABLE 2 Correlation between GWT and GCA area for each wetland at hourly, daily, monthly, and seasonal scales

Time scale	Hour	Day	Month	Season
Wetland 1	-0.2367	-0.2501	-0.3316	-0.3777
Wetland 2	-0.3236	-0.3723	-0.4848	-0.6132
Wetland 3	-0.7578	-0.7634	-0.8054	-0.8583
Wetland 4	-0.5246	-0.5268	-0.5745	-0.6116
Wetland 5	0.4194	0.4219	0.4420	0.5200
Wetland 6	-0.6010	-0.6032	-0.6394	-0.7389
Wetland 7	-0.4284	-0.4344	-0.5156	-0.7046
Wetland 8	-0.0515	-0.0516	-0.0625	-0.0468
Wetland 9	-0.1032	-0.1037	-0.1099	-0.2221
Wetland 10	-0.4538	-0.4557	-0.4907	-0.5032

wet and dry periods i.e., when the groundwater was shallower vs. when it was deeper, GCA generally exhibited very distinct response for each wetland. The absolute magnitude of correlations was lower than 0.5 only for wetlands 1, 8, and 9. At finer temporal scales, the absolute magnitude of correlations was much smaller. This was due to large fluctuations in GCA at shorter time scales even for small temporal variations in groundwater table height. It is worth noting that the correlation between GCA and GWT were generally negative for most, although not all, of the wetlands. The negative correlations, at least at the seasonal scale, indicated that GCA was smaller during wet periods and larger during dry periods.

Temporal variations in GCA were markedly different across wetlands even when the groundwater table (GWT) dynamics across them were similar. For example, the cross-correlations between the groundwater table in different wetlands were generally high at all considered temporal scales (Table S2). The average of cross-correlation of groundwater table between different wetlands at hourly, daily, monthly, and seasonal scales were 0.929, 0.929, 0.930, and 0.932, respectively. Range of cross-correlation values at different scales were [0.794, 0.996], [0.794, 0.996], [0.796, 0.996] and [0.800, 0.996], respectively. These results confirm close covariation of groundwater dynamics between wetlands in this watershed. However, the cross-correlations of GCA (see Table S3) varied from -0.46 (between wetland 4 and 5 for hourly time scale) to 0.81 (between wetland 5 and 8 for seasonal time scale), indicating disparate GCA response across wetlands. Here, the four seasons were defined to range from September–November (autumn), December– February (winter), March-May (spring), and June–August (summer).

The varied response of GCA, i.e., increase vs. decrease in GCA during dry periods, can be explained based on the conceptual model shown in Figure 5. The figure shows a schematic with two scenarios: scenario A (shown in the top) in which GCA during the dry period is larger than that in the wet period and scenario B (shown in the bottom) in which GCA during the dry period is smaller than in the wet period. In each of the two subfigures, a two-dimensional profile of groundwater table elevation around a representative wetland during both a dry and wet period (identified by GWT_t_{dry} and GWT_t_{wet} respectively) are shown. For the shown profiles, GCA for the wetland

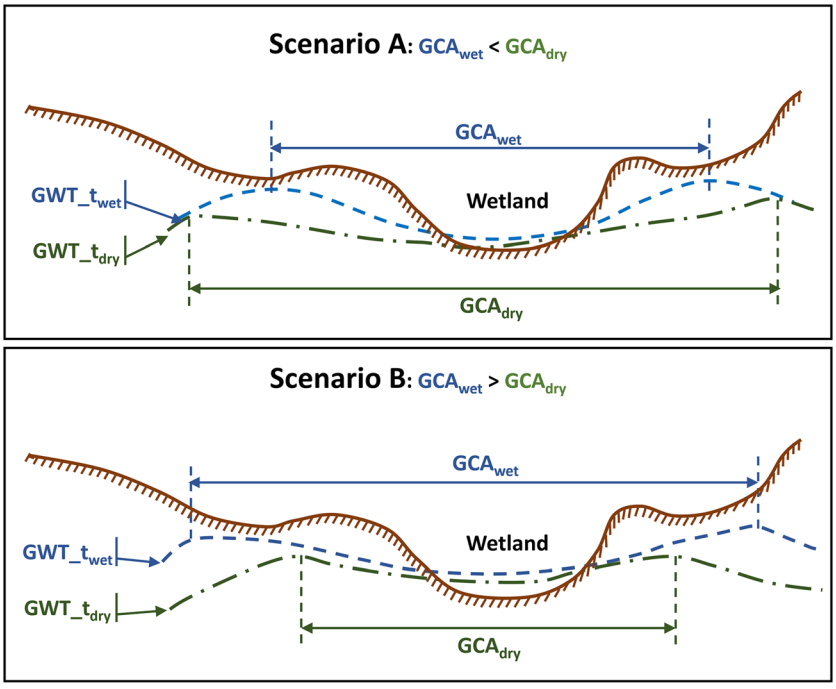

GWT_t_{wet}: groundwater table at time t_{wet} during wet period
GWT_t_{dry}: groundwater table at time t_{dry} during dry period
GCA_{wet}: groundwater contributing area at time t_{wet} during wet period
GCA_{dry}: groundwater contributing area at time t_{dry} during dry period

FIGURE 5 Conceptual model for groundwater contributing area (GCA) dynamics. Two scenarios are introduced to describe the variation in GCA between wet and dry periods. Scenario A shows a situation with larger contributing area in the dry period and scenario B presents a case with larger contributing area in the wet period

can be considered as the region between peaks of the groundwater table on either side of the wetland. Scenario A illustrates a situation when groundwater table just outside of GCA_{wet} boundary reduces by a smaller magnitude than at the groundwater boundary minus the difference in groundwater table elevation at the boundary and the outside of it. This results in groundwater table elevation in the dry period right outside of the GCA_{wet} boundary to be higher than at the boundary. Consequently, GCA increases in area during the dry period. As wetlands are generally situated in valleys and also experience high evapotranspiration rates, in part because the water in them is either directly exposed to the atmosphere or is easily accessible by the vegetation for transpiration, they facilitate loss of groundwater from the GCA. This results in a larger decrease in groundwater table at the GCA boundary during the dry period thus leading to a higher likelihood of increase in GCA for wetlands during the dry periods. However, as observed for wetland 5, it is always possible to have a positive correlation between GCA and GWT i.e., a decrease in GCA (instead of an increase) during the dry period, depending on the differences in hydrogeological properties, meteorological forcings, and bedrock gradient between inside and outside of the GCA. If the reduction in GWT at the GCA boundary is larger than inside of it plus the existing difference in groundwater table elevation at the boundary and the inside (see scenario B in Figure 5), GCA will become smaller in the dry period w.r.t. the wet period. It is to be noted that relative decrease/increase in GWT at the boundary of GCA does not have to happen all around the GCA circumference. A change just in a small section of the GCA boundary may extend/contract the GCA extent.

The two aforementioned scenarios explain the changes in the GCA between wet and dry periods as realized in the model simulation. This is demonstrated in Figure 6, which shows a GWT transect on a dry and wet date around wetlands 5 and 10. For wetland 5, the selected dry and wet dates are August 12 2006 (346^{th} day of 1^{st} year in Figure 4) and February 15 2006 (168^{th} day of 1^{st} year in Figure 4) respectively. The corresponding dates for wetland 10 are May 6 2008 (248^{th} day of 3^{rd} year in Figure 4) and August 29 2008 (364^{th} day of 3^{rd} year in Fig. 4). The dynamics of groundwater table around wetland 5 in Figure 6(c) indicates a situation that is presented in scenario B of Figure 5. Here, the groundwater table in the ninth element from point S (towards point E) experienced a decrease in elevation from 210.94 m to 210.28 m between the wet and the dry date, while the corresponding decrease in the eighth element was from 210.72 m to 210.45 m. This resulted in formation of groundwater divide at the edge of the eighth element on the dry date, which otherwise was far out at the edge of tenth element on the wet date. Similar formation of groundwater divides in other neighborhoods of wetland 5 as well resulted in the GCA to decrease from 2 km^2 on the wet date to 0.53 km^2 on the dry date. Scenario A is on exhibit in wetland 10 (Figure 6(d)) where the groundwater elevation in the eighth element increased from 239.80 m to 240.10 m between a dry and a wet date. The corresponding increase in elevation in the ninth element was from 239.82 m to 239.97 m. This results in contraction of groundwater divide from edge of element tenth to the edge of element eighth. As a result, the GCA for wetland 10 decreased from 3.89 km^2 on the dry date to 3.80 km^2 on the wet date.

4 | SUMMARY AND CONCLUSIONS

This study presents, to our knowledge, one of the first attempts at mapping the temporal dynamics of groundwater contributing area (GCA) of inland wetlands using a coupled surface-subsurface hydrologic model. GCA was computed for each model output time step (1 hr. in this case) using a multiple flow direction method. Although the mapping was performed on a model discretization with mixed grid shapes with both triangular and linear elements, the methodology can be applied to most other fully distributed models such as PARFLOW (Kollet & Maxwell, 2006), PAWS (Shen & Phanikumar, 2010), Hydrogeosphere (Therrien et al., 2010), CATHY (Camporese, Paniconi, Putti, & Orlandini, 2010), etc.

Our result demonstrates that GCAs for wetlands vary temporally, and are much different in extent and shape than the topographic contributing area (TCA). On average, GCAs varied by 0.162, 1.296, 14.197, and 23.995 % at hourly, daily, monthly, and seasonal intervals. This was much larger than variation in the average groundwater table in the wetlands, which was 0.007, 0.167, 4.268, and 10.382 % at the four temporal resolutions. The reason for higher frequency variation in GCA was because even small changes in the groundwater table at the boundary of GCA at a given time step could (dis/)connect with groundwater table in neighboring areas thus contracting/extending the GCA significantly. It is to be noted that abrupt changes in GCA may also occur as a result of merging of neighboring wetlands when the water table rises above the TCA boundary. However, given the distance between considered wetlands in the study area and the topographic relief within their TCA, this phenomenon was never realized in our simulations.

The results also showed that on an average GCAs were larger than TCA. This was true for more than 92% of the simulation period. As the groundwater-fed wetlands generally occurred within the flat convergence areas of the groundwater flow field, the smoother variations (lower spatial gradient) in groundwater flow field relative to the topography usually results in GCA being larger than the TCA. A larger GCA w.r.t. TCA indicated that water quality in wetlands might not only be contributed by contamination in its topographic contributing area, as is often considered in wetland quality estimation, restoration and preservation studies (Evenson, Golden, Lane, McLaughlin, & D'Amico, 2018; Hansen, Dolph, Foufoula-Georgiou, & Finlay, 2018; Russell, Hawkins, & O'Neill, 1997; Tomer, Tanner, & Howard-williams, 2009; White & Fennessy, 2005). Instead, water quality analyses should account for the contamination in the GCA, which may extend well beyond the TCA. Notably, the result is relevant only for wetlands that are (at least to some extent) groundwater-fed.

The difference in GCA and TCA may explain why (climate-)topographic metrics (e.g., Ali et al., 2014; Lang, McCarty, Oesterling, & Yeo, 2013; Merot et al., 2003) that are often used for identification/delineation/mapping of wetlands may fail in many settings. Notably,

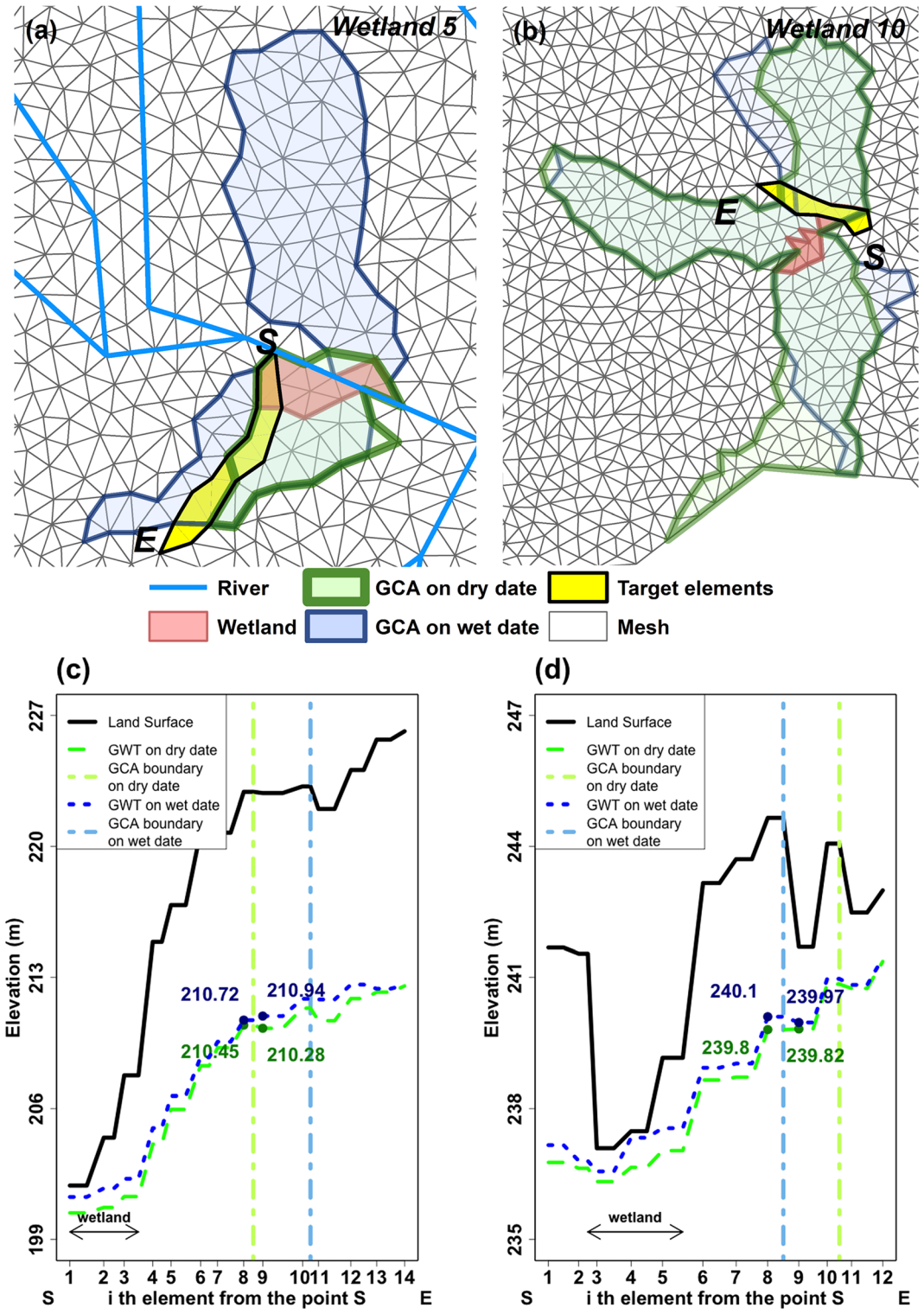

FIGURE 6 River, wetland, transition zone, topographic contributing area (TCA), and groundwater contributing area (GCA) on wet and dry dates for wetland 5 (a, top left) and wetland 10 (b, top right) respectively. Also shown are land surface elevation (black) and GWT (blue for the wet date, green for the dry date) in the transition zone around wetland 5 (c, bottom left) and wetland 10 (d, bottom right). Sky-blue and yellowgreen dashed vertical lines indicate the location of the GCA boundary on wet date and dry date, respectively. Transition zone consists of 14 and 12 discretization elements respectively around the boundary of GCA, with the center of the first element that is nearest to wetland being considered as the start (S) point

the said metrics do not account for the influence of temporally varying groundwater contributing area and consequently recharge to groundwater-fed wetlands. However, our result also showed that wetlands with larger TCA were likely to have larger GCA owing to topography's dominant role in determining the relative size of GCA over the landscape. This, after all, reaffirms that in spite of the simplicity of (climate-)topographic metrics, they may still have value for identification/delineation/mapping of wetlands.

All wetlands in the Second Creek watershed experienced similar precipitation, temperature and other meteorological forcings resulting in similar seasonal groundwater table (GWT) dynamics, but the GCA dynamics across some wetlands were markedly different. The correlation between GCA and GWT was generally found to be negative for most of the wetlands. The overall negative correlations at the seasonal scale indicated that GCA was smaller during wet periods and larger during dry periods for most of the wetlands. However, one wetland did show a positive correlation between GCA and GWT. To explain the disparate temporal dynamics of GCAs across wetlands that lie within the same hydroclimatic setting, a conceptual model based on the relative changes in groundwater table elevation at the boundary of GCA and its neighbor was developed. The model explained the cause for why GCA across different wetlands may either increase or decrease. The conceptual model may be used in future studies to identify *a priori* if GCA for a wetland will be larger during wet period w.r.t. the dry periods. The timing could be useful for delineation of maximum GCA, using a transient groundwater well network.

Although hydroclimatic conditions are shown to strongly influence GCA dynamics as indicated by the temporal variations in GCA, our results show that they are also controlled by physiographic factors that result in disparate variations in GCA across the wetlands even when they occur within the same hydroclimate. Despite the fact that majority of the wetlands in the watershed show an overall negative correlation between GCA and GWT dynamics, in part due to the efficiency of the wetlands and its surrounding landscape for losing groundwater through evapotranspiration, it is possible for these correlations to be either positive or negative depending on the spatial distribution of physiographic and hydrogeological properties. Future studies focused on GCA mapping of wetlands in watersheds with disparate hydrologic properties will help confirm if certain organization of watershed properties generally result in higher incidence of negative correlation between GCA and GWT for inland wetlands. While previous studies have highlighted the role of surface and subsurface flux exchange between the wetland and the neighboring aquifer, river, and hillslope on groundwater dynamics in wetlands (Bertassello et al., 2018; Frei, Lischeid, & Fleckenstein, 2010; Scheliga, Tetzlaff, Nuetzmann, & Soulsby, 2019; D. Wang et al., 2018), the results here show that GCA dynamics is also sensitive to groundwater flow field that lie away from the wetland.

Although the simulated hydrologic responses, specifically the streamflow response near the watershed outlet and the groundwater table dynamics at the gauge location, were previously validated, more confidence in the simulated extent and shape of GCA dynamics can be gained by performing groundwater table measurements at fine spatiotemporal resolutions around each wetland. The simulated GCA map may likely have been affected by the parameterization used in the model domain and the mesh configuration. Notably, simulations conducted using alternative mesh resolution may yield different GCA extent even when the groundwater table dynamics is similar. This is due to the dependence of GCA on local differences in groundwater table height in neighboring elements, which can suddenly (dis-)connect large areas to the existing GCA. If the goal is to map out GCA for decision making, it is suggested that a fine enough mesh resolution be chosen such that the GCA dynamics is independent of the mesh resolution at any finer scale while still ensuring that simulations remain computationally tractable. In spite of the aforementioned uncertainties, the study highlights the disparate dynamics of GCA in space and time across wetlands within a watershed. The results could be used to guide source area estimation of wetland contamination, prediction of wetland locations, and understanding the resilience of wetlands. The result may also help guide the design of groundwater well observation network needed to understand the dynamics of the flow field that recharges wetlands.

ACKNOWLEDGMENT

Authors acknowledge support from National Science Foundation grants EAR-1856054 and EAR-1920425.

CONFLICT OF INTEREST

The authors have no conflict of interest to declare.

DATA AVAILABILITY STATEMENT

The data that support the findings of this study are available from the corresponding author upon reasonable request.

ORCID

Junehyeong Park https://orcid.org/0000-0001-7806-4803
Mukesh Kumar https://orcid.org/0000-0001-7114-9978

REFERENCE

Abdelbaki, A. M. (2016). Using automatic calibration method for optimizing the performance of Pedotransfer functions of saturated hydraulic conductivity. *Ain Shams Engineering Journal*, *7*(2), 653–662. https://doi.org/10.1016/j.asej.2015.05.012

Ali, G., Birkel, C., Tetzlaff, D., Soulsby, C., McDonnell, J. J., & Tarolli, P. (2014). A comparison of wetness indices for the prediction of observed connected saturated areas under contrasting conditions. *Earth Surface Processes and Landforms*, *39*(3), 399–413. https://doi.org/10.1002/esp.3506

Ameli, A. A., & Creed, I. F. (2017). Quantifying hydrologic connectivity of wetlands to surface water systems. *Hydrology and Earth System Sciences*, *21*(3), 1791–1808. https://doi.org/10.5194/hess-21-1791-2017

Barbier, E. B. (1993). Sustainable Use of Wetlands Valuing Tropical Wetland Benefits: Economic Methodologies and Applications. *The Geographical Journal*, *159*(1), 22. https://doi.org/10.2307/3451486

Benson, C. E., Carberry, B., & Langen, T. A. (2018). Public–private partnership wetland restoration programs benefit Species of Greatest Conservation Need and other wetland-associated wildlife. *Wetlands Ecology and Management*, *26*(2), 195–211. https://doi.org/10.1007/s11273-017-9565-8

Bertassello, L. E., Rao, P. S. C., Park, J., Jawitz, J. W., & Botter, G. (2018). Stochastic modeling of wetland-groundwater systems. *Advances in Water Resources*, *112*, 214–223. https://doi.org/10.1016/J.ADVWATRES.2017.12.007

Bhatt, G., Kumar, M., & Duffy, C. J. (2014). A tightly coupled GIS and distributed hydrologic modeling framework. *Environmental Modelling & Software*, *62*, 70–84. https://doi.org/10.1016/j.envsoft.2014.08.003

Bullock, A., & Acreman, M. (2003). The role of wetlands in the hydrological cycle. *Hydrology and Earth System Sciences*, *7*(3), 358–389. https://doi.org/10.5194/hess-7-358-2003

Camporese, M., Paniconi, C., Putti, M., & Orlandini, S. (2010). Surface-subsurface flow modeling with path-based runoff routing, boundary condition-based coupling, and assimilation of multisource observation data. *Water Resources Research*, *46*(2), W02512. https://doi.org/10.1029/2008WR007536

Chen, X., Kumar, M., & McGlynn, B. L. (2015). Variations in Streamflow Response to Large Hurricane-Season Storms in a Southeastern U.S. Watershed. *Journal of Hydrometeorology*, *16*(1), 55–69. https://doi.org/10.1175/JHM-D-14-0044.1

Chen, X., Kumar, M., Wang, R., Winstral, A., & Marks, D. (2016). Assessment of the Timing of Daily Peak Streamflow during the Melt Season in a Snow-Dominated Watershed. *Journal of Hydrometeorology*, *17*(8), 2225–2244. https://doi.org/10.1175/JHM-D-15-0152.1

Chu, X., Yang, J., Chi, Y., & Zhang, J. (2013). Dynamic puddle delineation and modeling of puddle-to-puddle filling-spilling-merging-splitting overland flow processes. *Water Resources Research*, *49*(6), 3825–3829. https://doi.org/10.1002/wrcr.20286

Daniel, C. C. (1987). Statistical analysis relating well yield to construction practices and siting of wells in the Piedmont and Blue Ridge provinces of North Carolina. *Water-Resources Investigations Report*. https://doi.org/10.3133/wri864132

Erwin, K. L. (2009). Wetlands and global climate change: the role of wetland restoration in a changing world. *Wetlands Ecology and Management*, *17*(1), 71–84. https://doi.org/10.1007/s11273-008-9119-1

Evenson, G. R., Golden, H. E., Lane, C. R., McLaughlin, D. L., & D'Amico, E. (2018). Depressional wetlands affect watershed hydrological, biogeochemical, and ecological functions. *Ecological Applications*, *28*(4), 953–966. https://doi.org/10.1002/eap.1701

Fossey, M., & Rousseau, A. N. (2016). Can isolated and riparian wetlands mitigate the impact of climate change on watershed hydrology? A case study approach. *Journal of Environmental Management*, *184*(Pt 2), 327–339. https://doi.org/10.1016/j.jenvman.2016.09.043

Freeman, T. G. (1991). Calculating catchment area with divergent flow based on a regular grid. *Computers & Geosciences*, *17*(3), 413–422. https://doi.org/10.1016/0098-3004(91)90048-I

Frei, S., Lischeid, G., & Fleckenstein, J. H. (2010). Effects of micro-topography on surface-subsurface exchange and runoff generation in a virtual riparian wetland - A modeling study. *Advances in Water Resources*, *33*(11), 1388–1401. https://doi.org/10.1016/j.advwatres.2010.07.006

Galat, D. L., Fredrickson, L. H., Humburg, D. D., Bataille, K. J., Bodie, J. R., Dohrenwend, J., … Semlitsch, R. D. (1998). Flooding to Restore Connectivity of Regulated, Large-River Wetlands. *BioScience*, *48*(9), 721–733. https://doi.org/10.2307/1313335

Gesch, D. B., Oimoen, M. J., Greenlee, S. K., Nelson, C. A., Steuck, M. J., & Tyler, D. J. (2002). The national elevation data set. *Photogrammetric Engineering and Remote Sensing*, *68*(1), 5–11. Retrieved from. http://pubs.er.usgs.gov/publication/70156331

Gilliam, J. W. (1994). Riparian Wetlands and Water Quality. *Journal of Environment Quality*, *23*(5), 896. https://doi.org/10.2134/jeq1994.00472425002300050007x

Hansen, A. T., Dolph, C. L., Foufoula-Georgiou, E., & Finlay, J. C. (2018). Contribution of wetlands to nitrate removal at the watershed scale. *Nature Geoscience*, *11*(2), 127–132. https://doi.org/10.1038/s41561-017-0056-6

Harbaugh, A. W. (2005). *MODFLOW-2005: the U.S. Geological Survey modular ground-water model--the ground-water flow process* (No. 6-A16). https://doi.org/10.3133/TM6A16

Harbor, J. M. (1994). A Practical Method for Estimating the Impact of Land-Use Change on Surface Runoff, Groundwater Recharge and Wetland Hydrology. *Journal of the American Planning Association*, *60*(1), 95–108. https://doi.org/10.1080/01944369408975555

Hey, D. L., & Philippi, N. S. (1995). Flood Reduction through Wetland Restoration: The Upper Mississippi River Basin as a Case History. *Restoration Ecology*, *3*(1), 4–17. https://doi.org/10.1111/j.1526-100X.1995.tb00070.x

Homer, C., Dewitz, J., Yang, L., Jin, S., Danielson, P., Xian, G., … Megown, K. (2015). Completion of the 2011 National Land Cover Database for the Conterminous United States - Representing a Decade of Land Cover Change Information. In *Photogrammetric Engineering and Remote Sensing* (Vol. 81). https://doi.org/10.14358/PERS.81.5.345

Hunt, R. J., Krabbenhoft, D. P., & Anderson, M. P. (1996). Groundwater Inflow Measurements in Wetland Systems. *Water Resources Research*, *32*(3), 495–507. https://doi.org/10.1029/95WR03724

Hwang, H.-T., Park, Y.-J., Sudicky, E. A., & Forsyth, P. A. (2014). A parallel computational framework to solve flow and transport in integrated surface–subsurface hydrologic systems. *Environmental Modelling & Software*, *61*, 39–58. https://doi.org/10.1016/J.ENVSOFT.2014.06.024

Jolly, I. D., McEwan, K. L., & Holland, K. L. (2008). A review of groundwater-surface water interactions in arid/semi-arid wetlands and the consequences of salinity for wetland ecology. *Ecohydrology*, *1*(1), 43–58. https://doi.org/10.1002/eco.6

Jordan, T. E., Whigham, D. F., Hofmockel, K. H., & Pittek, M. A. (2003). Nutrient and Sediment Removal by a Restored Wetland Receiving Agricultural Runoff. *Journal of Environment Quality*, *32*(4), 1534. https://doi.org/10.2134/jeq2003.1534

van der Kamp, G., & Hayashi, M. (2009). Groundwater-wetland ecosystem interaction in the semiarid glaciated plains of North America. *Hydrogeology Journal*, *17*(1), 203–214. https://doi.org/10.1007/s10040-008-0367-1

Knight, R. L. (1997). Wildlife habitat and public use benefits of treatment wetlands. *Water Science and Technology*, *35*(5), 35–43. https://doi.org/10.1016/S0273-1223(97)00050-4

Knight, R. L., Clarke, R. A., & Bastian, R. K. (2001). Surface flow (SF) treatment wetlands as a habitat for wildlife and humans. *Water Science and Technology*, *44*(11–12), 27–37. https://doi.org/10.2166/wst.2001.0806

Kollet, S. J., & Maxwell, R. M. (2006). Integrated surface–groundwater flow modeling: A free-surface overland flow boundary condition in a parallel groundwater flow model. *Advances in Water Resources*, *29*(7), 945–958. https://doi.org/10.1016/J.ADVWATRES.2005.08.006

Kottek, M., Grieser, J., Beck, C., Rudolf, B., & Rubel, F. (2006). World Map of the Köppen-Geiger climate classification updated. *Meteorologische Zeitschrift*, *15*(3), 259–263. https://doi.org/10.1127/0941-2948/2006/0130

Krapu, C., Kumar, M., & Borsuk, M. (2018). Identifying Wetland Consolidation Using Remote Sensing in the North Dakota Prairie Pothole Region. *Water Resources Research*, *54*(10), 7478–7494. https://doi.org/10.1029/2018WR023338

Kumar, M. (2009). *Toward a Hydrologic Modeling System*. The Pennsylvania State University.

Kumar, M., Bhatt, G., & Duffy, C. J. (2009). An efficient domain decomposition framework for accurate representation of geodata in distributed hydrologic models. *International Journal of Geographical Information Science*, *23*(12), 1569–1596. https://doi.org/10.1080/13658810802344143

Kumar, M., Bhatt, G., & Duffy, C. J. (2010). An object-oriented shared data model for GIS and distributed hydrologic models. *International Journal of Geographical Information Science*, *24*(7), 1061–1079. https://doi.org/10.1080/13658810903289460

Kumar, M., & Duffy, C. J. (2015). Exploring the Role of Domain Partitioning on Efficiency of Parallel Distributed Hydrologic Model Simulations. *Journal of Hydrogeology and Hydrologic Engineering*, *04*(01). https://doi.org/10.4172/2325-9647.1000119

Kumar, M., Duffy, C. J., & Salvage, K. M. (2009). A Second-Order Accurate, Finite Volume–Based, Integrated Hydrologic Modeling (FIHM) Framework for Simulation of Surface and Subsurface Flow. *Vadose Zone Journal*, *8*(4), 873. https://doi.org/10.2136/vzj2009.0014

Kumar, M., Marks, D., Dozier, J., Reba, M., & Winstral, A. (2013). Evaluation of distributed hydrologic impacts of temperature-index and energy-based snow models. *Advances in Water Resources*, *56*, 77–89. https://doi.org/10.1016/J.ADVWATRES.2013.03.006

Lang, M., McCarty, G., Oesterling, R., & Yeo, I.-Y. (2013). Topographic Metrics for Improved Mapping of Forested Wetlands. *Wetlands*, *33*(1), 141–155. https://doi.org/10.1007/s13157-012-0359-8

Lin, Y.-F., Jing, S.-R., Wang, T.-W., & Lee, D.-Y. (2002). Effects of macrophytes and external carbon sources on nitrate removal from groundwater in constructed wetlands. *Environmental Pollution*, *119*(3), 413–420. https://doi.org/10.1016/S0269-7491(01)00299-8

Liu, Y., & Kumar, M. (2016). Role of meteorological controls on interannual variations in wet-period characteristics of wetlands. *Water Resources Research*, *52*(7), 5056–5074. https://doi.org/10.1002/2015WR018493

Locke, R. A. I., Miner, J. J., Sinclair, S. V, Anliker, M. A., Pociask, G. E., Robinson, B. J., & Dey, W. S. (2005). *A Method for Estimating Groundwater Contribution Areas by Illinois State Water Survey* (No. 2005–11). Champaign, IL.

McCarthy, T. S. (2006). Groundwater in the wetlands of the Okavango Delta, Botswana, and its contribution to the structure and function of the ecosystem. *Journal of Hydrology*, *320*(3–4), 264–282. https://doi.org/10.1016/J.JHYDROL.2005.07.045

Merot, P., Squividant, H., Aurousseau, P., Hefting, M., Burt, T., Maitre, V., … Viaud, V. (2003). Testing a climato-topographic index for predicting wetlands distribution along an European climate gradient. *Ecological Modelling*, *163*(1–2), 51–71. https://doi.org/10.1016/S0304-3800(02)00387-3

Min, J.-H., Perkins, D. B., & Jawitz, J. W. (2010). Wetland-Groundwater Interactions in Subtropical Depressional Wetlands. *Wetlands*, *30*(5), 997–1006. https://doi.org/10.1007/s13157-010-0043-9

Misut, P. E., & Monti, J. J. (2016). *Delineation of areas contributing groundwater to selected receiving surface water bodies for long-term average hydrologic conditions from 1968 to 1983 for Long Island, New York* (No. 2016–5138). https://doi.org/10.3133/sir20165138

Mitsch, W. J., & Gosselink, J. G. (2000). The value of wetlands: importance of scale and landscape setting. *Ecological Economics*, *35*(1), 25–33. https://doi.org/10.1016/S0921-8009(00)00165-8

Mungur, A. S., Shutes, R. B. E., Revitt, D. M., & House, M. A. (1995). An assessment of metal removal from highway runoff by a natural wetland. *Water Science and Technology*, *32*(3), 169–175. https://doi.org/10.1016/0273-1223(95)00617-6

National Research Council. (1995). *Wetlands: Characteristics and Boundaries*. https://doi.org/10.17226/4766

Nippgen, F., Mcglynn, B. L., & Emanuel, R. E. (2015). The spatial and temporal evolution of contributing areas. *Water Resources Research*, *51*, 4550–4573. https://doi.org/10.1002/2014WR016719

O'Driscoll, M. A., & Parizek, R. R. (2003). The hydrologic catchment area of a chain of karst wetlands in central Pennsylvania, USA. *Wetlands*, *23*(1), 171–179. https://doi.org/10.1672/0277-5212(2003)023[0171:thcaoa]2.0.co;2

Park, J., Botter, G., Jawitz, J. W., & Rao, P. S. C. (2014). Stochastic modeling of hydrologic variability of geographically isolated wetlands: Effects of hydro-climatic forcing and wetland bathymetry. *Advances in Water Resources*, *69*, 38–48. https://doi.org/10.1016/J.ADVWATRES.2014.03.007

Pollock, D. W. (2012). *User guide for MODPATH version 6 - A particle-tracking model for MODFLOW* (No. 6-A41). https://doi.org/10.3133/TM6A41

Qu, Y., & Duffy, C. J. (2007). A semidiscrete finite volume formulation for multiprocess watershed simulation. *Water Resources Research*, *43*(8), W08419. https://doi.org/10.1029/2006WR005752

Quinn, P., Beven, K., Chevallier, P., & Planchon, O. (1991). The prediction of hillslope flow paths for distributed hydrological modelling using digital terrain models. *Hydrological Processes*, *5*(1), 59–79. https://doi.org/10.1002/hyp.3360050106

Reuter, J. E., Djohan, T., & Goldman, C. R. (1992). The use of wetlands for nutrient removal from surface runoff in a cold climate region of california—results from a newly constructed wetland at lake tahoe. *Journal of Environmental Management*, *36*(1), 35–53. https://doi.org/10.1016/S0301-4797(05)80100-8

Richardson, C. J. (1994). Ecological functions and human values in wetlands: A framework for assessing forestry impacts. *Wetlands*, *14*(1), 1–9. https://doi.org/10.1007/BF03160616

Rodríguez-Lado, L., Rial, M., Taboada, T., & Cortizas, A. M. (2015). A Pedotransfer Function to Map Soil Bulk Density from Limited Data. *Procedia Environmental Sciences*, *27*, 45–48. https://doi.org/10.1016/j.proenv.2015.07.112

Russell, G. D., Hawkins, C. P., & O'Neill, M. P. (1997). The Role of GIS in Selecting Sites for Riparian Restoration Based on Hyderology and Land Use. *Restoration Ecology*, *5*, 56–68. https://doi.org/10.1111/j.1526-100X.1997.tb00205.x

Scheliga, B., Tetzlaff, D., Nuetzmann, G., & Soulsby, C. (2019). Assessing runoff generation in riparian wetlands: monitoring groundwater–surface water dynamics at the micro-catchment scale. *Environmental Monitoring and Assessment*, *191*(2). https://doi.org/10.1007/s10661-019-7237-2

Seo, S. B., Sinha, T., Mahinthakumar, G., Sankarasubramanian, A., & Kumar, M. (2016). Identification of dominant source of errors in developing streamflow and groundwater projections under near-term climate change. *Journal of Geophysical Research: Atmospheres*, *121*(13), 7652–7672. https://doi.org/10.1002/2016JD025138

Shaw, D. A., Vanderkamp, G., Conly, F. M., Pietroniro, A., & Martz, L. (2012). The Fill-Spill Hydrology of Prairie Wetland Complexes during Drought and Deluge. *Hydrological Processes*, *26*(20), 3147–3156. https://doi.org/10.1002/hyp.8390

Shen, C., & Phanikumar, M. S. (2010). A process-based, distributed hydrologic model based on a large-scale method for surface–subsurface coupling. *Advances in Water Resources*, *33*(12), 1524–1541. https://doi.org/10.1016/J.ADVWATRES.2010.09.002

Soil Survey Staff, Natural Resources Conservation Service, U. S. D. of A. (2005). Soil Survey Geographic (SSURGO) Database. Retrieved from https://sdmdataaccess.sc.egov.usda.gov

Therrien, R., McLaren, R. G., Sudicky, E. A., & Panday, S. M. (2010). *HydroGeoSphere. A three-dimensional numerical model describing fully-integrated subsurface and surface flow and solute transport*. https://doi.org/10.5123/S1679-49742014000300002

Tomer, M., Tanner, C., & Howard-williams, C. (2009). Discussing Wetlands, Agriculture, and Ecosystem Services. *Wetland Science and Practice*, *26*(4), 26–29. https://doi.org/10.1672/055.026.0407

U.S. Fish and Wildlife Service. (2019). National Wetlands Inventory. Retrieved April 20, 2019, from https://www.fws.gov/wetlands/

Van Meter, K. J., & Basu, N. B. (2015). Signatures of human impact: size distributions and spatial organization of wetlands in the Prairie Pothole landscape. *Ecological Applications*, *25*(2), 451–465. https://doi.org/10.1890/14-0662.1

Vanderhoof, M. K., Alexander, L. C., & Todd, M. J. (2016). Temporal and spatial patterns of wetland extent influence variability of surface water connectivity in the Prairie Pothole Region, United States. *Landscape Ecology*, *31*(4), 805–824. https://doi.org/10.1007/s10980-015-0290-5

Vivoni, E. R., Ivanov, V. Y., Bras, R. L., & Entekhabi, D. (2004). Generation of Triangulated Irregular Networks Based on Hydrological Similarity. *Journal of Hydrologic Engineering*, *9*(4), 288–302. https://doi.org/10.1061/(ASCE)1084-0699(2004)9:4(288)

Vivoni, E. R., Mascaro, G., Mniszewski, S., Fasel, P., Springer, E. P., Ivanov, V. Y., & Bras, R. L. (2011). Real-world hydrologic assessment of a fully-distributed hydrological model in a parallel computing environment. *Journal of Hydrology*, *409*(1–2), 483–496. https://doi.org/10.1016/J.JHYDROL.2011.08.053

Wang, D., Liu, Y., & Kumar, M. (2018). Using nested discretization for a detailed yet computationally efficient simulation of local hydrology in a distributed hydrologic model. *Scientific Reports*, *8*(1), 1–11. https://doi.org/10.1038/s41598-018-24122-7

Wang, R., Kumar, M., & Marks, D. (2013). Anomalous trend in soil evaporation in a semi-arid, snow-dominated watershed. *Advances in Water Resources*, *57*, 32–40. https://doi.org/10.1016/J.ADVWATRES.2013.03.004

Watson, K. B., Ricketts, T., Galford, G., Polasky, S., & O'Niel-Dunne, J. (2016). Quantifying flood mitigation services: The economic value of Otter Creek wetlands and floodplains to Middlebury, VT. *Ecological Economics*, *130*, 16–24. https://doi.org/10.1016/J.ECOLECON.2016.05.015

White, D., & Fennessy, S. (2005). Modeling the suitability of wetland restoration potential at the watershed scale. *Ecological Engineering*, *24*(4), 359–377. https://doi.org/10.1016/J.ECOLENG.2005.01.012

Winter, T. C. (1999). Relation of streams, lakes, and wetlands to groundwater flow systems. *Hydrogeology Journal*, *7*(1), 28–45. https://doi.org/10.1007/s100400050178

Wösten, J. H. M., Pachepsky, Y. A., & Rawls, W. J. (2001). Pedotransfer functions: Bridging the gap between available basic soil data and missing soil hydraulic characteristics. *Journal of Hydrology*, *251*(3–4), 123–150. https://doi.org/10.1016/S0022-1694(01)00464-4

Xia, Y., Mitchell, K., Ek, M., Sheffield, J., Cosgrove, B., Wood, E., … Mocko, D. (2012). Continental-scale water and energy flux analysis and validation for the North American Land Data Assimilation System project phase 2 (NLDAS-2): 1. Intercomparison and application of model products. *Journal of Geophysical Research: Atmospheres*, *117*, D03109. https://doi.org/10.1029/2011JD016048

Yang, J., & Chu, X. (2013). Quantification of the spatio-temporal variations in hydrologic connectivity of small-scale topographic surfaces under various rainfall conditions. *Journal of Hydrology*, *505*, 65–77. https://doi.org/10.1016/J.JHYDROL.2013.09.013

Yu, X., Bhatt, G., Duffy, C., Wardrop, D., Najjar, R., Ross, A., & Rydzik, M. (2015). A coupled surface–subsurface modeling framework to assess the impact of climate change on freshwater wetlands. *Climate Research*, *66*(3), 211–228. https://doi.org/10.3354/cr01348

Yu, X., Duffy, C., Baldwin, D. C., & Lin, H. (2014). The role of macropores and multi-resolution soil survey datasets for distributed surface–subsurface flow modeling. *Journal of Hydrology*, *516*, 97–106. https://doi.org/10.1016/J.JHYDROL.2014.02.055

Zedler, J. B., & Kercher, S. (2005). WETLAND RESOURCES: Status, Trends, Ecosystem Services, and Restorability. *Annual Review of Environment and Resources*, *30*(1), 39–74. https://doi.org/10.1146/annurev.energy.30.050504.144248

Zhang, M., Chen, X., Kumar, M., Marani, M., & Goralczyk, M. (2017). Hurricanes and tropical storms: A necessary evil to ensure water supply? *Hydrological Processes*, *31*(24), 4414–4428. https://doi.org/10.1002/hyp.11371

Zhu, J., Sun, G., Li, W., Zhang, Y., Miao, G., Noormets, A., … Wang, X. (2017). Modeling the potential impacts of climate change on the water table level of selected forested wetlands in the southeastern United States. *Hydrology and Earth System Sciences*, *21*(12), 6289–6305. https://doi.org/10.5194/hess-21-6289-2017

SUPPORTING INFORMATION

Additional supporting information may be found online in the Supporting Information section at the end of this article.

Table S1: Wetland type and attributes based on the National Wetland Inventory (NWI) for the ten selected wetland used in this study. All these wetlands are classified as Palustrine wetlands. Multiple rows for a given wetland indicate existence of several NWI polygon features within it.

Table S2: Cross correlation between GWT in different wetlands at hourly, daily, monthly, and seasonal scales

Table S3: Cross correlation between GCA for different wetlands at hourly, daily, monthly, and seasonal scales

How to cite this article: Park J, Wang D, Kumar M. Spatial and temporal variations in the groundwater contributing areas of inland wetlands. *Hydrological Processes*. 2019;1–14. https://doi.org/10.1002/hyp.13652